The New Year Wave: Spatial Evolution of an Extreme Sea State

Günther F. Clauss

Marco Klein[1]
e-mail: klein@naoe.tu-berlin.de

Ocean Engineering Division,
Technical University Berlin,
Salzufer 17-19,
10587 Berlin, Germany

In the past years the existence of freak waves has been affirmed by observations, registrations, and severe accidents. Many publications investigated the occurrence of extreme waves, their characteristics and their impact on offshore structures, but their formation process is still under discussion. One of the famous real world registrations is the so called "New Year wave," recorded in the North Sea at the Draupner jacket platform on January 1st, 1995. Since there is only a single point registration available, it is not possible to draw conclusions on the spatial development in front of and behind the point of registration, which is indispensable for a complete understanding of this phenomenon. This paper presents the spatial development of the New Year wave generated in a model basin. To transfer the recorded New Year wave into the wave tank, an optimization approach for the experimental generation of wave sequences with predefined characteristics is applied. The extreme sea state obtained with this method is measured at different locations in the tank, in a range from 2163 m (full scale) ahead of to 1470 m behind the target position—520 registrations altogether. The focus lies on the detailed description of a possible evolution of the New Year wave over a large area and time interval. It is observed that the extreme wave at the target position develops mainly from a wave group of three smaller waves. The group velocity, wave propagation, and the energy flux of this wave group are analyzed, in particular. [DOI: 10.1115/1.3160533]

1 Introduction

One of the most famous freak waves in history is the so called New Year wave, recorded in the North Sea at the Draupner jacket platform on January 1st, 1995 [1]. Numerous other observations, registrations, or dangerous encounters confirm the reality of freak waves. Freak waves are reported from the Japanese Sea [2], the Norwegian Frigg field [3], and from the Danish Gorm field [4]. Guedes Soares et al. [5] presented investigations from the North Cormoran field as well as sea state measurements taken during hurricane Camille [6]. Furthermore, Wolfram et al. [7] analyzed storm data recorded from 1994 to 1998 at North Alwyn, discovering 21 freak waves (higher than $2 \cdot H_s$) in a 5 day storm (Nov. 16–21, 1997). In addition, there are reports from cruise vessels encountering freak waves, such as the *Bremen* (February, 2001) [8], the *Voyager* (February, 2005) [9] and the *Norwegian Dawn* (April, 2005) [10]. The impact on offshore structures is also under investigation. Gorf et al. [11] investigated the bow damage of a floating production, storage and offloading vessel (FPSO) in steep waves, revealing that wave steepness is an important parameter. Clauss et al. [12,13] presented comprehensive studies on the vertical bending moments of a FPSO due to rogue wave impact, comparing numerical simulations and model tests, including the generation of deterministic wave sequences with embedded rogue waves as a critical prerequisite [14]. The realization of freak waves in deterministic seakeeping tests was introduced by Kühnlein [15] and refined by Kühnlein et al. [16] by taking nonlinear wave-wave interaction into account. An optimization approach for the generation of user-defined freak waves embedded in irregular sea states was introduced by Clauss and Schmittner [17]. Many publications have been investigating the formation process of freak waves, and although different physical mechanisms have already been identified, this issue is still under discussion. Since only a single point registration is available, it is not possible to draw conclusions on the spatial development in front of and behind the measurement point. Buchner et al. [18] presented the evolution of an extreme wave at different positions in a model basin, revealing that the extreme wave develops in less than half the wavelength from a relatively normal wave into an extreme crest. Inspired by this approach, this paper presents a spatial development of the New Year wave generated in a model basin ($L = 120$ m, $W = 8$ m, $d = 1$ m, scale of 1:70). The surface elevation of the extreme sea state is successively measured along the tank, in a range from 2163 m (full scale) ahead to 1470 m behind the target position—at 520 locations altogether.

Section 2 gives a short summary of established wave theories and Sec. 3 illustrates the procedure of irregular wave train generation with the embedded New Year wave. Subsequently, the experimental setup and the results of the extensive measurements are presented.

2 Wave Propagation and Wave Generation

The controversy arising on the formation process of freak waves in the past decades reveals that the physical background is still not completely solved. The possible physical mechanisms have already been identified—superposition of (nonlinear) component waves and/or modulation instability. The phenomenon of freak waves occurring due to wave-current interaction is ignored in this discussion as this mechanism is well understood and explainable by linear theory [19]—in contrast to the sudden occurrence of exceptionally high waves. In the following a short summary of established wave theories is given, without any claim of completeness.

The genesis of the established theories is based on the comprehensive studies of Stokes [20]. The Stokes wave theory solves the Laplace equation including the nonlinear boundary conditions by a perturbation method, which enables an approximate solution of the boundary value problem. The basic solution of the Stokes expansion is the well known linear wave theory. Expansions of velocity potential and wave elevation are leading to Stokes third order solutions (e.g., Ref. [21]). These solutions take nonlinearities such as the increase in propagation speed due to wave steepness and the increase in crest-trough asymmetry into account.

[1]Corresponding author.

Contributed by the Ocean Offshore and Arctic Engineering Division of ASME for publication in the JOURNAL OF OFFSHORE MECHANICS AND ARCTIC ENGINEERING. Manuscript received October 6, 2008; final manuscript received May 7, 2009; published online October 1, 2009. Assoc. Editor: Takeshi Kinoshita. Paper presented at the ASME 27th International Conference on Offshore Mechanics and Arctic Engineering (OMAE2008), Estoril, Portugal, June 15–20, 2008.

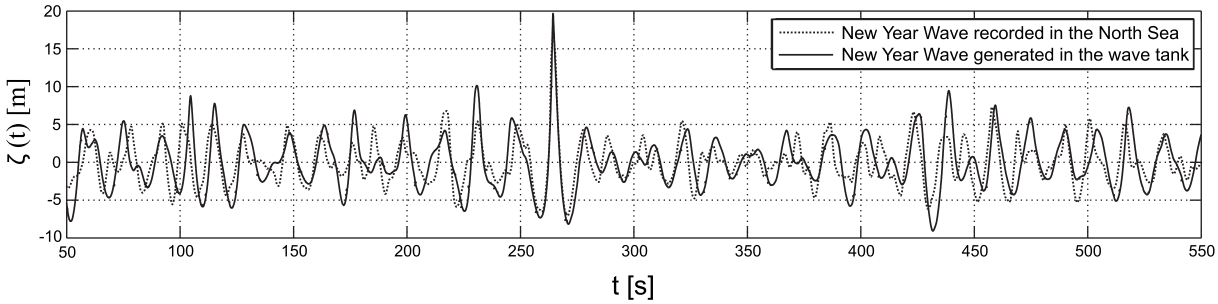

Fig. 1 Comparison of measured model wave train at target position (scale of 1:70) and the sequence recorded at the Draupner platform (all data full scale)

Benjamin and Feir [22] investigated the stability of periodic wave trains (Stokes waves) with small disturbances caused by a pair of side-band modes. This investigation reveals that weakly nonlinear deepwater wave trains are unstable to modulational perturbations due to the coupling through the nonlinear boundary conditions. The instability condition $0<\delta\leq\sqrt{2}k\zeta_a$ has later been introduced as the Benjamin–Feir-index (BFI), and a relation between spectral bandwidth δ and wave steepness $k\zeta_a$ has been established by Janssen [23] and Onorato et al. [24]. Further investigations show that the time evolution of weakly nonlinear deep water wave trains can be expressed by the nonlinear Schrödinger (NLS) equation [25,26], which has been solved exactly by Zakharov and Shabat [27]. This solution predicts the existence of deep water wave envelope solitons, which has been verified by experiments [28]. Dysthe [29] introduced a fourth-order modified nonlinear Schrödinger (MNLS) equation for gravity waves and infinite water depth. The application of the NLS equation and the Benjamin–Feir instability to rogue wave crests and troughs (holes) in deep water wave trains has been shown by Osborne et al. [30]. The results above are well understood, and robust from the physical [31] as well as the mathematical [32,33] point of view. Nevertheless, it remains unclear how realistic wave sequences (broad bandwidth) with embedded rogue waves can be generated by applying the Benjamin–Feir instability, since the NLS equation is limited in terms of bandwidth [34,35]. Hence, for the generation and investigation of the spatial development of an extreme sea state, a "standard model of ocean waves" [36] is used to generate tailored wave sequences with integrated freak waves by controlled superposition. The method for generating linear wave groups is based on the wave focusing technique by Davis and Zarnick [37] and its significant enhancement by Takezawa and Hirayama [38]. The generation of higher and steeper wave sequences requires a more sophisticated approach as propagation velocity increases with height. As the associated wave sequence propagates according to nonlinear wave theory, it is not possible to calculate the wave train linearly upstream back to the wave generator in order to determine the control signal of the wave board. To solve this problem, Kühnlein [15] developed a semi-empirical procedure for the evolution of extremely high wave groups, based on linear wave theory. With this deterministic technique, freak waves of up to 3.2 m height have been generated in a wave tank [39]. Generally (for wave groups as well as irregular seas with embedded rogue wave sequences), substantial deviations between the measured time series and the specified design wave train at the target location are registered if a linearly synthesized control signal is used for the generation of higher and steeper waves. The main deviation, however, is localized within a small range, proving that only a short section of the control signal in time domain has to be adapted [40].

In Sec. 3 the optimization approach for the experimental generation of tailored wave sequences with predefined characteristics according to Clauss and Schmittner [17] is briefly described.

3 Generation of The New Year Wave

For the investigation of the spatial development of an extreme sea state, the New Year wave, recorded at the Draupner platform in the North Sea on January 1st, 1995 [1] is chosen. This giant single wave ($H_{max}=25.63$ m) with a crest height of $\zeta_c=18.5$ m occurred in a surrounding sea state characterized by a significant wave height of $H_s=11.92$ m ($H_{max}/H_s=2.15$) at a water depth of $d\approx 70$ m. The measurements are conducted in the seakeeping basin of the Ocean Engineering Division, Technical University Berlin, at a model scale of 1:70. The total length of the basin is 110 m long, with an effective measuring length of 90 m. The width is 8 m, and the water depth is 1 m, which represents—with the chosen model scale—the actual water depth at the Draupner jacket platform. To transfer the recorded wave into the wave tank, an optimization approach for the experimental generation of tailored wave sequences with predefined characteristics is used [14,17]. This method enables the generation of scenarios with a single high wave superimposed to irregular seas. During the experimental optimization special emphasis is laid on the exact reproduction of the wave height, crest height, wave period, as well as the vertical and horizontal asymmetries of the target wave. At the beginning of the optimization process, the scaled real-sea measured sea state is transformed back to the position of the piston type wave generator by means of linear wave theory. By multiplication with the electrical and hydrodynamic transfer functions in the frequency domain and the subsequent inverse Fourier transformation, a preliminary control signal for the wave generator is obtained. Since this control signal is based on linear theory, nonlinear effects such as wave/wave interaction and wave breaking are neglected. Due to nonlinear effects in the wave tank, the registration of the wave sequence at the target position generated by the preliminary control signal deviates from the predefined target parameters. As aforementioned, only a short section of the control signal in the

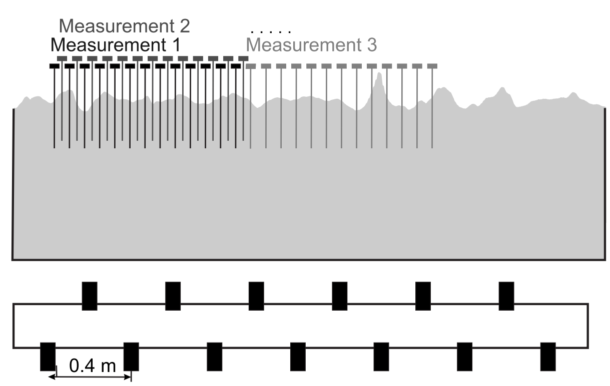

Fig. 2 Schematic sketch of the experimental setup

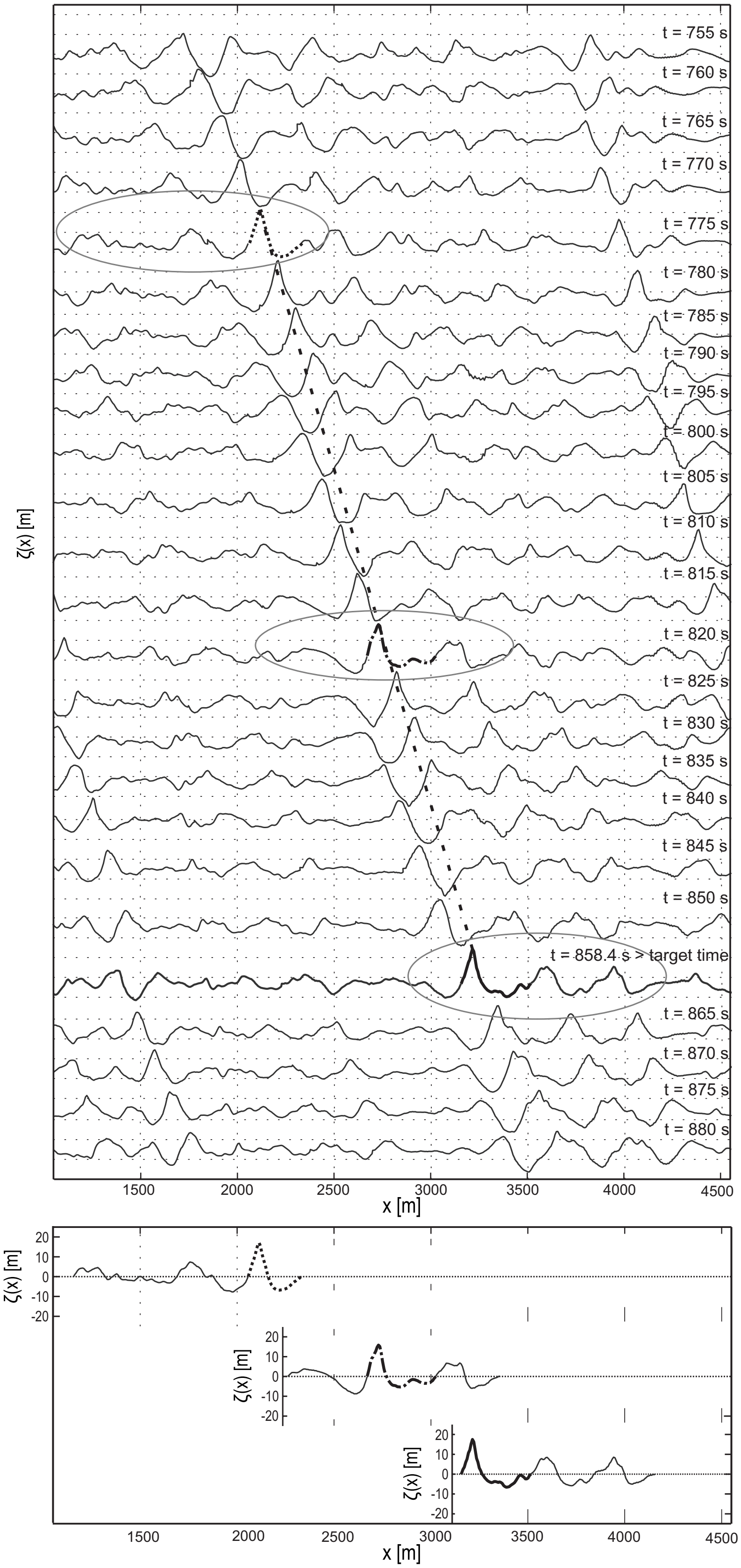

Fig. 3 Spatial development of the extreme sea state for selected time steps (full scale)

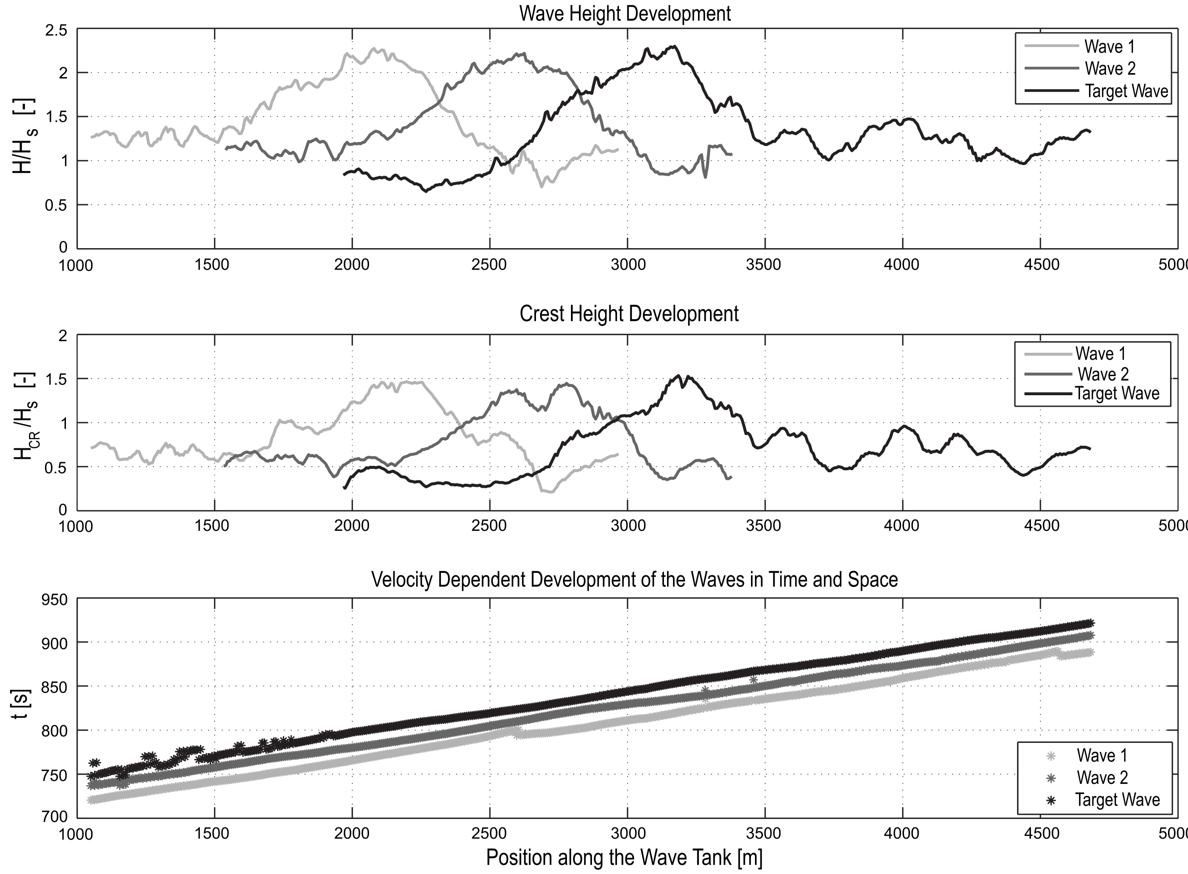

Fig. 4 Progress of the wave heights along the wave tank and velocity-dependent development of the wave crests in time and space

time domain has to be adapted to satisfy the target parameters of the extreme wave. For these (temporally limited) local changes in the control signal, the discrete wavelet transformation [41] is introduced into the optimization process. This transformation samples the signal into several decomposition levels where each resulting coefficient describes the wave in a specific time range and frequency bandwidth. To improve the control signal, the experimental optimization routine iterates until the target parameters are satisfied. The adaptation of the wave train is achieved by applying the subplex optimization method [42]. Since the values of the target function are determined from the wave tank experiment, real-world nonlinear free surface effects are included in the adoption procedure, resulting in a "self-validating" process. Figure 1 shows the measurement of the wave tank in comparison to the original wave sequence recorded at the Draupner platform.

4 Experimental Setup

The wave measurements are conducted in the seakeeping basin (length $L=120$ m, breadth $W=8$ m, and water depth $d=1$ m) of the Technical University Berlin at a model scale of 1:70. The spatial development of the New Year wave is measured in a range from 2163 m (full scale) ahead of to 1470 m behind the target position by a total of 520 registrations. The towing carriage is equipped with 13 wave gauges installed at an interval of 0.2 m and the wave tank is subdivided into 20 measurement sections. To achieve a resolution of $\Delta x=0.1$ m, two measurements per area are carried out: at position x and $x+\Delta x$, respectively. Figure 2 shows the experimental setup schematically, with a side view on the setup (top) describing the measurement order as well as a top view on the arrangement of the wave gauges installed on the towing carriage (bottom).

5 Results

Figure 3 presents the surface elevations measured in the wave tank for selected time steps (full scale). Surprisingly, the analysis of the registrations reveals freak waves occurring at three different positions in the wave tank (dotted line ($t\approx 775$ s), dash-dotted line C_{crest} and solid bold line ($t\approx 858$ s)). At $t\approx 858$ s, a snapshot of the New Year wave at target time in the wave tank is shown. Note that the observed freak waves are developing from a wave group of three waves (encircled in Fig. 3 (top)), which travels with constant speed along the wave tank up to the target position. The lower diagram shows the wave group at the moments of freak wave occurrences in detail. Figure 4 illustrates the progress of the wave heights along the wave tank and the propagation velocity (celerity) of the three waves. The top diagram shows the ratio of wave height to significant wave height of the surrounding sea state. Here, the occurrence of the three freak waves is clearly identifiable. The first wave reaches its maximum height at 2110 m,

Table 1 Summary of the main characteristics of the three freak waves

	Wave 1	Wave 2	Target wave
$H_{\max}$ (m)	26.82	26.46	27.41
$H_{\max}/H_s$	2.25	2.22	2.29
$\zeta_{c_{\max}}$ (m)	17.28	17.22	18.15
$\zeta_{c_{\max}}/H_s$	1.45	1.44	1.52
C_{crest} (m/s)	23.34	21.42	21.31
T_0 (s)	≈16	≈16	≈16

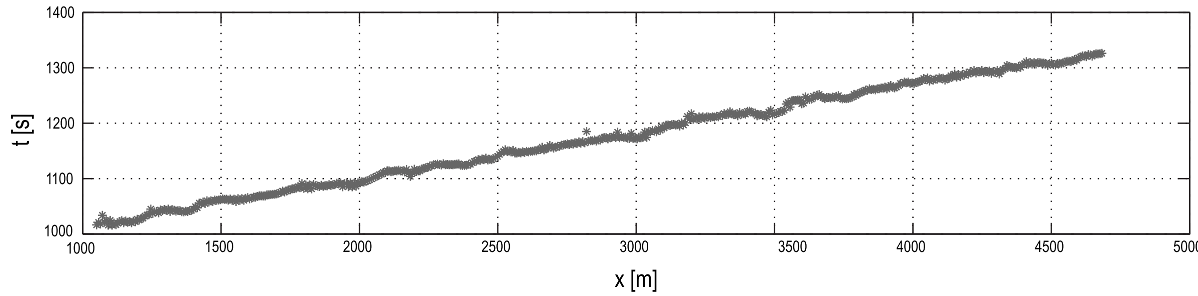

Fig. 5 Progress of the centroid of the mean energy distribution $\bar{E}$ for registrations at each location

the second at 2624 m, and the target wave at 3213 m distance from the wave maker. The distance between these maximum waves remains almost constant (514 m between waves 1 and 2; 589 m between wave 2 and the target wave). Note that the two waves occurring in front of the wave group are temporarily high waves as well ($H=19.6$ m and 23.1 m). The distance between the locations of occurrence of the maximum wave height for these two waves and the locations of the maximum wave height of the following freak waves are also almost constant (≈ 500 m). It seems that the first freak wave develops from wave components of the two waves in front of the wave group. Due to the approximately constant propagation velocity of the three waves in the wave group, the following freak waves seem to develop from these wave components as well. In the following, the three observed freak waves are investigated in detail.

All three waves show the same genesis: The wave height increases continuously over a range of 550–630 m. In addition, the first two extreme waves ($H/H_s>2$) are propagating over a wide range (280–360 m), whereas the target wave ($H/H_s>2$) propagates the shortest distance. This is due to the fact that the New Year wave (in contrast to the first two freak waves) is breaking behind the target location. The center diagram of Fig. 4 presents the ratio of wave crest height to significant wave height. Finally, the lower diagram presents the time and space coherence of the three wave crests along the wave tank: This diagram reveals that the wave crests propagate almost in parallel and approximately constant through the wave tank. The linear regression of the set of points results in the crest velocities of the three waves: $C_{\text{crest}_1}=21.34$ m/s, $C_{\text{crest}_2}=21.42$ m/s and $C_{\text{crest}_{\text{target}}}=21.31$ m/s. In summary, Fig. 4 shows that all three freak waves feature almost identical characteristics (see Table 1).

Furthermore, Table 1 displays the mean zero-upcrossing periods of the three waves, which are oscillating between $T_{\text{up}_{\min}} \approx 14$ s and $T_{\text{up}_{\max}} \approx 18$ s, resulting in a mean period of $T_0 \approx 16$ s for the three waves during their propagation along the

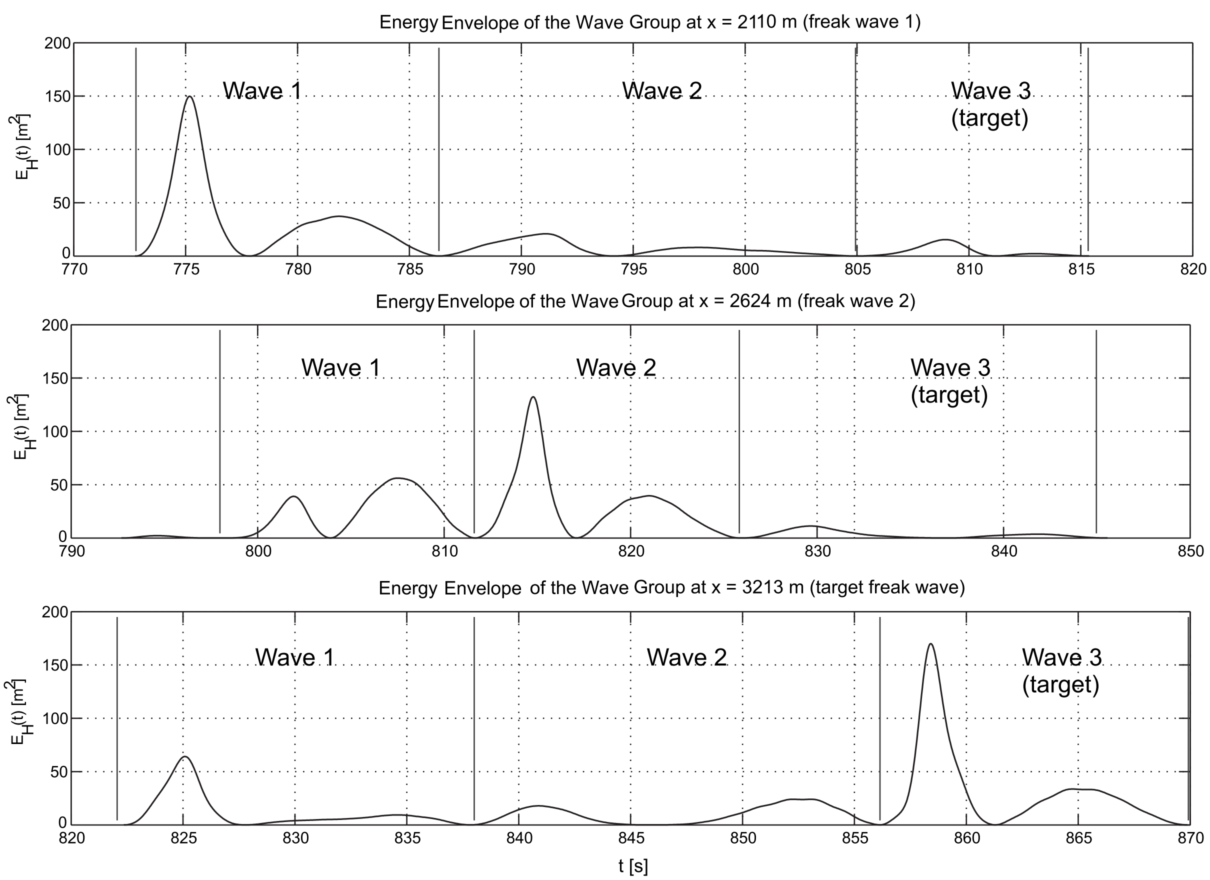

Fig. 6 Energy envelope for the wave group at different locations in the tank

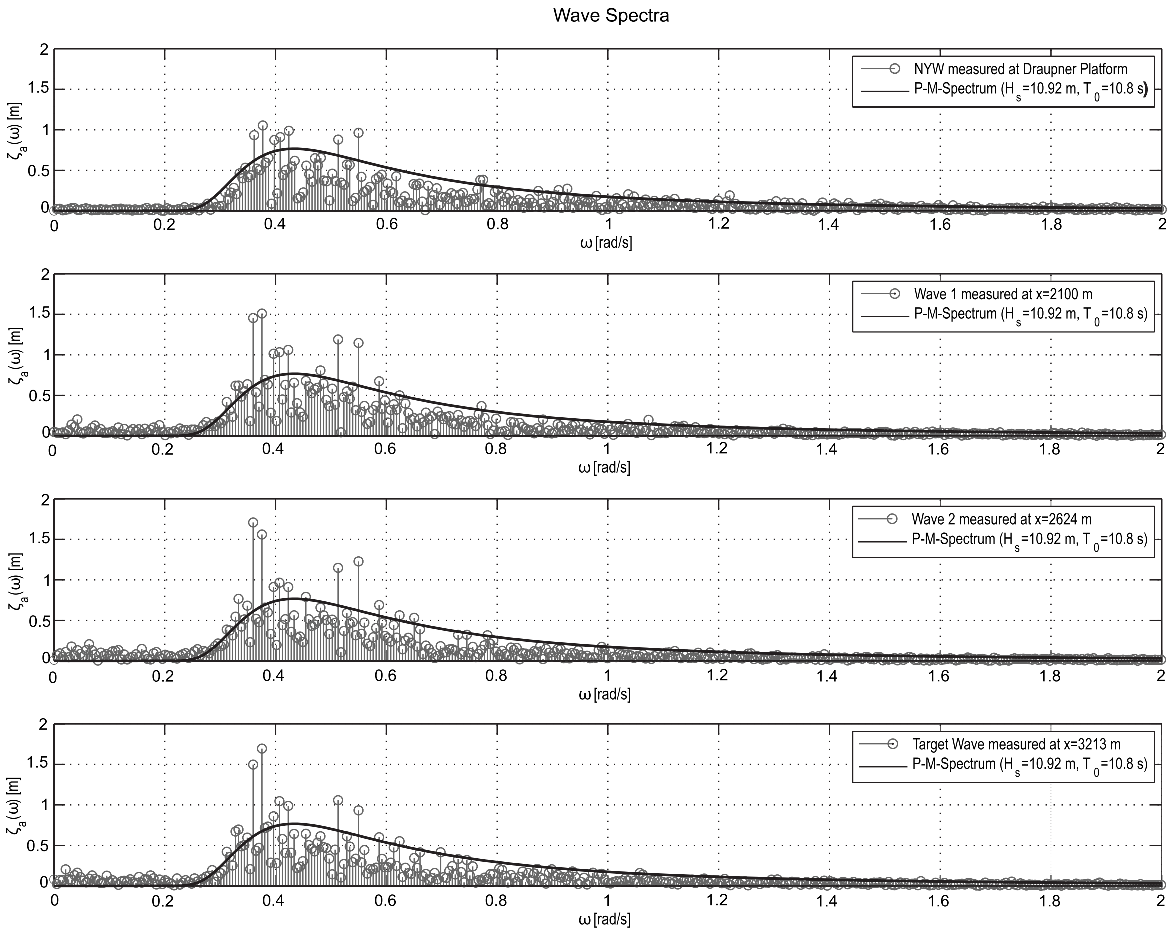

Fig. 7 Comparison of the wave spectra of the New Year wave and the model wave sequences at different locations (the locations of occurrence of the three freak waves)

tank. With $T_p \approx 16.7$ s, the peak period of the surrounding sea state is close to the mean wave periods of the three waves. So far, the individual waves observed are growing and shrinking in time and space. If the propagation velocity of the highest wave elevation is analyzed (which is attributed to different individual waves) we identify its position in time and space along the bold dashed line in Fig. 3. Evaluating the propagation speed of this highest elevation, we obtain $C_{\text{crest}_{\text{freak}}} \approx 13$ m/s, which is about half of the wave celerity, and corresponds to the group velocity, describing the energy propagation.

For evaluating the mean velocity of energy propagation, the time-dependent progress of the centroid $c_{\text{med}}(t,x)$ of the mean energy distribution $\bar{E}(t,x)$,

$$c_{\text{med}}(t,x) = \frac{\sum \bar{E}_i(t,x) \cdot c_{\text{med}_i}(t,x)}{\sum \bar{E}_i(t,x)} \tag{1}$$

with

$$\bar{E}_i = \frac{1}{2}\rho g \zeta_i^2 \tag{2}$$

is calculated at each location along the wave tank, which is illustrated in Fig. 5. Linear regression results in the mean velocity of energy propagation $C_{\bar{E}} = 11.73$ m/s.

Based on this result, the energy of the wave group is investigated in detail. Using the time-varying energy envelope concept [43], the energy envelope $E_H(t)$ of the wave group ζ_{WG} can be described using the Hilbert transformation technique.

$$E_H(x,t) = \frac{1}{2}|\hat{\zeta}(x,t)|^2 = \frac{1}{2}[\zeta_{\text{WG}}^2(x,t) + \zeta_H^2(x,t)] \tag{3}$$

where ζ_H is the real part of the Hilbert transformation of ζ_{WG}. Figure 6 illustrates energy envelopes at different locations. Similar to the mean velocity of energy propagation and the velocity of the highest elevation, the energy of the wave group propagates with $C_{\text{gr}} \approx C_{\text{crest}}/2$, i.e., with half of the celerity. The focusing of the wave group energy beneath the freak wave at the target position becomes clearly visible. Finally the wave spectra and asymmetry are investigated in detail. Figure 7 presents the comparison of the wave spectra of the New Year wave and the registrations in the wave tank at the locations of occurrence of the three freak waves. All spectra are compared with the Pierson–Moskovitz-spectrum of $H_s = 11.92$ m and $T_0 = 10.8$ s, showing good agreement.

Figure 8 presents the crest front steepness ϵ of the three waves during their development along the wave tank as defined by Kjeldsen [44] (Fig. 8 (bottom)).

$$\epsilon = \frac{\zeta_c}{L'} \tag{4}$$

Typically wave breaking occurs within a range of $\epsilon = 0.32 - 0.78$, where the highest values are associated with plunging breakers [45]. The upper three diagrams show the development of the crest front steepness of the three extremely high waves (note that the respective time axes are different). The development of the crest front steepness of the target wave can be divided into three sections: At the beginning of the wave formation the crest front steepness is low but increases rapidly at $t \approx 830$ s and finally

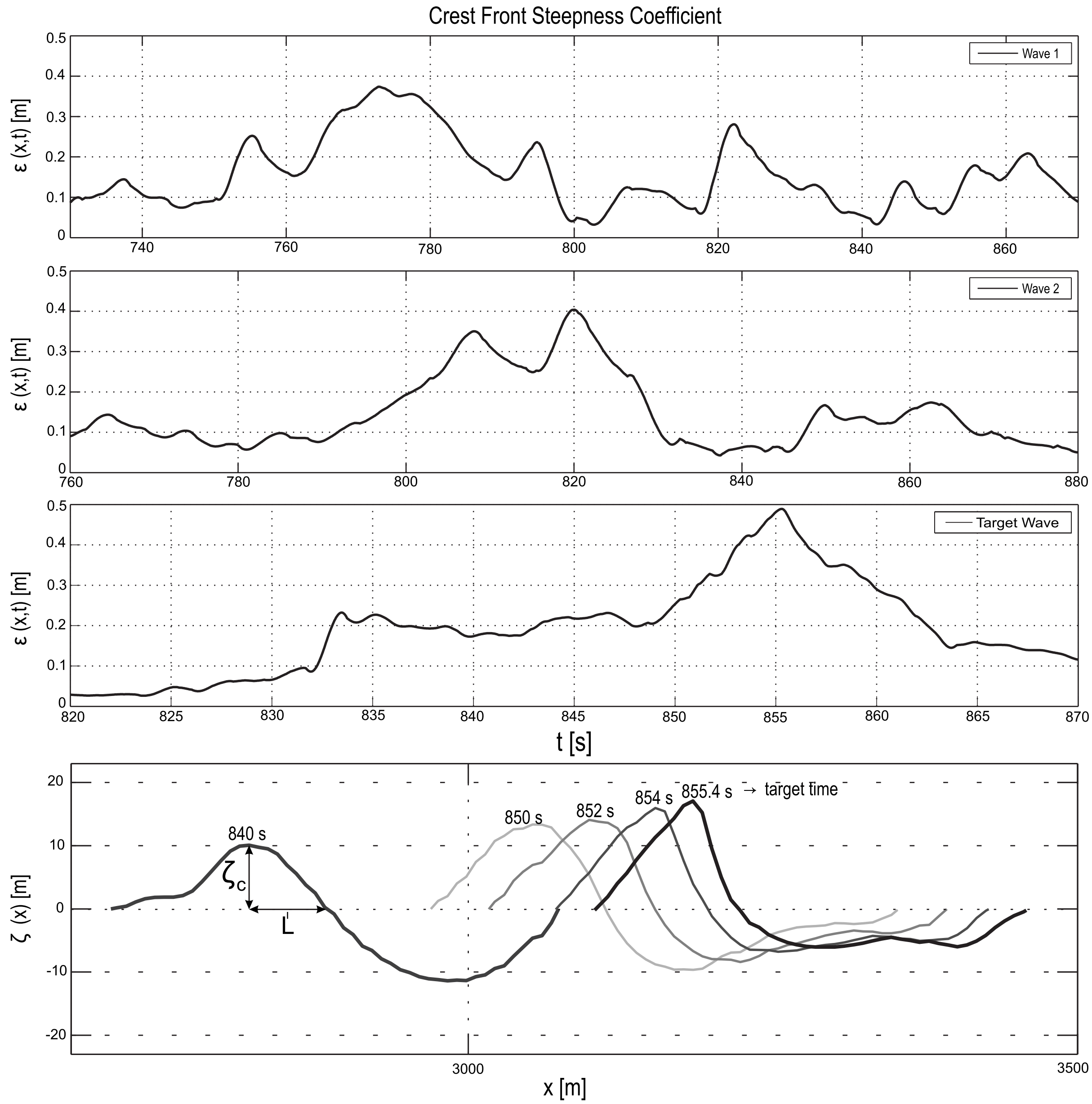

Fig. 8 Crest front steepness of the three waves as defined by Kjeldsen [42] (upper three diagrams). Snapshots of the target wave for different time steps (bottom).

reaches its maximum value ϵ=0.49 at target location. Note that the crest front steepness of waves 1 and 2 (ϵ_1=0.37 and ϵ_2=0.4) are also within the typical breaking limits [44]. This corresponds to observations during the wave tank measurements, where the target wave is breaking as a plunging breaker after the target location, whereas waves 1 and 2 were identified as waves with white crests. The bottom diagram in Fig. 8 shows snapshots of the target wave for different time steps: The increase in the crest front steepness is clearly identifiable, since the crest height ζ_c increases while the length L' decreases.

6 Conclusions

This paper presents a comprehensive study of the spatial evolution of an extreme sea state with an embedded rogue wave. The New Year wave, recorded at the Draupner platform in the North Sea on January 1st, 1995 [1], has been generated in the wave tank at scale of 1:70 and is measured at different locations in the tank, in a range from 2163 m (full scale) ahead of to 1470 m behind the target position.

Surprisingly, the analysis of the registrations revealed freak waves occurring at three different positions in the wave tank. It is shown that the three observed freak waves emerge from a wave group, which propagates almost constantly along the wave tank. The two waves in front of the wave group are quite high waves as well (H=19.6 m and 23.1 m). The distance between the locations of occurrence of the maximum wave height for these two waves and the locations of maximum wave height of the following freak waves are nearly constant (≈500 m). Further investigations reveal that all three freak waves feature similar statistical characteristics (see Table. 1).

The investigation of crest front steepness shows that all three freak waves are within the breaking wave domain proposed by Kjeldsen [44].

The analysis of the total energy propagation shows that the wave crest velocity of the three waves in the wave group is almost twice the velocity of the mean energy, which results in the temporarily occurrence of the three freak waves at different wave crests. For these freak waves the focusing of the wave group energy at the target position is shown.

Acknowledgment

This paper is published as a contribution to the project "Handling Waves," which is founded by the European Commission, under the Contract No. TST5-CT-2006-031489. We highly acknowledge the support of this research project.

Nomenclature

C_{crest} = crest celerity
$C_{\bar{E}}$ = velocity of mean energy propagation
C_{gr} = group velocity
$\bar{E}$ = mean energy distribution
E_H = energy envelope
H = wave height
$H_{\max}$ = maximum wave height
H_s = significant wave height
L = length
L' = horizontal distance between the wave crest and the zero-upcrossing point
T_0 = zero-upcrossing period
W = wave tank breadth
Δx = spatial resolution
c_{med} = mean energy distribution centroid
d = water depth
g = gravitational acceleration
k = wave number
δ = spectral bandwidth
ϵ = crest front steepness
ρ = density
ζ = wave elevation
$\hat{\zeta}$ = complex analytical signal
ζ_a = wave amplitude
ζ_c = wave crest height
ζ_H = real part of the Hilbert transformation
ζ_{WG} = wave group elevation

References

[1] Haver, S., and Anderson, O. J., 2000, "Freak Waves: Rare Realization of a Typical Population or Typical Realization of a Rare Population?," *Proceedings of the Tenth International Offshore and Polar Engineering Conference (ISOPE)*, Seattle, WA, pp. 123–130.
[2] Mori, N., Yasuda, T., and Nakayama, S., 2000, "Statistical Properties of Freak Waves Observed in the Sea of Japan," *Proceedings of the Tenth International Offshore and Polar Engineering Conference (ISOPE)*, Seattle, WA, Vol. 3, pp. 109–122.
[3] Kjeldsen, S. P., 1990, "Breaking Waves," *Proceedings of the NATO Advanced Research Workshop on Water Wave Kinematics*, A. Tørum and O. Gudmestad, eds., Kluwer Academic, Molde, Norway, pp. 453–473.
[4] Sand, S. E., Ottesen Hansen, N. E., Klinting, P., Gudmestad, O. T., and Sterndorff, M. J., 1989, "Freak Wave Kinematics", *Water Wave Kinematics*, Kluwer Academic, NATO ASI Series, pp. 535–549.
[5] Guedes Soares, C., Cherneva, Z., and Antão, E. M., 2004, "Characteristics of Abnormal Waves in North Sea Storm Sea States," Appl. Ocean. Res., **25**, pp. 337–344.
[6] Guedes Soares, C., Cherneva, Z., and Antão, E. M., 2004, "Abnormal Waves During Hurricane Camille," J. Geophys. Res., [Oceans], **109**, pp. C08008.1–C08008.7.
[7] Wolfram, J., Linfoot, B., and Stansell, P., 2000, "Long- and Short-Term Extreme Wave Statistics in the North Sea: 1994–1998," Rogue Waves 2000, Brest, France, pp. 363–372.
[8] Schulz, M., 2001, "Ich spürte den Atem Gottes," Der Spiegel, No. 51/2001.
[9] Bertotti, L., and Cavaleri, L., 2008, "Analysis of the Voyager Storm," Ocean Eng., **35**(1), pp. 1–5.
[10] Lemire, J., 2005, "Freak Wave Rocks Cruise," http://www.cbmu.com/news.php?articleID=228.
[11] Gorf, P., Barltrop, N., Okan, B., Hodgson, T., and Rainey, R., 2000, "FPSO Bow Damage in Steep Waves," Rogue Waves 2000, Brest, France.
[12] Clauss, G. F., Schmittner, C. E., Hennig, J., Guedes Soares, C., Fonseca, N., and Pascoal, R., 2004, "Bending Moments of an FPSO in Rogue Waves," OMAE 2004—23rd International Conference on Offshore Mechanics and Arctic Engineering, Vancouver, Canada, Paper No. oMAE2004-51504.
[13] Clauss, G. F., Kauffeldt, A., and Jacobsen, K., 2007, "Longitudinal Forces and Bending Moments of a FPSO," OMAE 2007—26th International Conference on Offshore Mechanics and Arctic Engineering, San Diego, CA, Paper No. oMAE2007-29091.
[14] Clauss, G. F., 2008, "The Taming of the Shrew: Tailoring Freak Wave Sequences for Seakeeping Tests," J. Ship Res., **52**(3), pp. 194–226, www.naoe.tuberlin.de/MT.
[15] Kühnlein, W., 1997, "Seegangsversuchstechnik mit transienter Systemanregung," Ph.D. thesis, Technische Universität Berlin, Berlin, Germany.
[16] Kühnlein, W., Clauss, G., and Hennig, J., 2002, "Tailor Made Freak Waves Within Irregular Seas," OMAE 2002—21st Conference on Offshore Mechanics and Arctic Engineering, Oslo, Norway, Paper No. oMAE2002-28524.
[17] Clauss, G. F., and Schmittner, C. E., 2005, "Experimental Optimization of Extreme Wave Sequences for the Deterministic Analysis of Wave/Structure Interaction," OMAE 2005—24th International Conference on Offshore Mechanics and Arctic Engineering, Halkidiki, Greece, Paper No. oMAE2005-67049.
[18] Buchner, B., van Dijk, R., and Voogt, A., 2007, "The Spatial Analysis of an Extreme Wave in a Model Basin," OMAE 2007—26th International Conference on Offshore Mechanics and Arctic Engineering, San Diego, CA, Paper No. oMAE2007-29409.
[19] Trulsen, K., and Dysthe, K. B., 1997, "Freak Waves—A Three-Dimensional Wave Simulation," *Proceedings of the 21st Symposium on Naval Hydrodynamics*, Washington, DC, pp. 550–560.
[20] Stokes, G. G., 1849, "On the Theory of Oscillatory Waves," Trans. Cambridge Philos. Soc., **8**, pp. 441–455.
[21] Kinsman, B., 1965, *Wind Waves*, Prentice-Hall, Englewood Cliffs, NJ.
[22] Benjamin, T., and Feir, J., 1967, "The Disintegration of Wave Trains on Deep Water," J. Fluid Mech., **27**(3), pp. 417–430.
[23] Janssen, P., 2003, "Nonlinear Four-Wave Interactions and Freak Waves," J. Phys. Oceanogr., **33**, pp. 863–884.
[24] Onorato, M., Osborne, A. R., Serio, M., Cavaleri, L., Brandini, C., and Stansberg, C. T., 2003, "Extreme Waves and Modulational Instability: Wave Flume Experiments on Irregular Waves," ArXiv Nonlinear Sciences e-prints.
[25] Zakharov, V. E., 1968, "Stability of Periodic Waves of Finite Amplitude on the Surface of a Deep Fluid," J. Appl. Mech. Tech. Phys., **9**, pp. 190–194.
[26] Hasimoto, H., and Ono, H., 1972, "Nonlinear Modulation of Gravity Waves," J. Phys. Soc. Jpn., **33**, pp. 805–811.
[27] Zakharov, V. E., and Shabat, A. B., 1971, "Exact Theory of Two-Dimensional Self-Focusing and One-Dimensional Self-Modulating Waves in Nonlinear Media," Sov. Phys. JETP, **2**, pp. 118–134.
[28] Yuen, H. C., and Lake, B. M., 1975, "Nonlinear Deep Water Waves: Theory and Experiments," Phys. Fluids, **18**, pp. 956–960.
[29] Dysthe, K. B., 1979, "Note on a Modification to the Nonlinear Schrödinger Equation for Application to Deep Water Waves," Proc. R. Soc. London, Ser. A, **A369**, pp. 105–114.
[30] Osborne, A. R., Onorato, M., and Serio, M., 2000, "The Nonlinear Dynamics of Rogue Waves and Holes in Deep-Water Gravity Wave Trains," Phys. Lett. A, **275**, pp. 386–393.
[31] Yuen, H., 1991, "Recent Advances in Nonlinear Water Waves: An Overview," *Nonlinear Topics in Ocean Physics*, A. R. Osborne, ed., North-Holland, Amsterdam, pp. 461–498.
[32] Its, A. R., and Kotljarov, V. P., 1976, "Explicit Formulas for Solutions of a Nonlinear Schrödinger Equation," Seriya A. Fiziko-Matematicheskie i Tekhnicheskie Nauki, **1051**, pp. 965–968.
[33] Tracy, E. R., and Chen, H. H., 1988, "Nonlinear Self-Modulation: An Exactly Solvable Model," Phys. Rev. A, **37**(3), pp. 815–839.
[34] Onorato, M., Osborne, A. R., Serio, M., and Bertone, S., 2001, "Freak Waves in Random Oceanic Sea States," Phys. Rev. Lett., **86**(25), pp. 5831–5834.
[35] Trulsen, K., and Dysthe, K. B., 1996, "A Modified Nonlinear Schrödinger Equation for Broader Bandwidth Gravity Waves on Deep Water," Wave Motion, **24**, pp. 281–289.
[36] Forristall, G. Z., 2005, "Understanding Rogue Waves: Are New Physics Really Necessary?," Rogue Waves 14th 'Aha Huliko'a Hawaiian Winter Workshop, University of Hawaii, Manoa, Honolulu, http://www.soest.hawaii.edu/PubServices/AhaHulikoa.html.
[37] Davis, M., and Zarnick, E., 1964, "Testing Ship Models in Transient Waves," Fifth Symposium on Naval Hydrodynamics.
[38] Takezawa, S., and Hirayama, T., 1976, "Advanced Experimental Techniques for Testing Ship Models in Transient Water Waves. Part II: The Controlled Transient Water Waves for Using in Ship Motion Tests," *Proceedings of the 11th Symposium on Naval Hydrodynamics: Unsteady Hydrodynamics of Marine Vehicles*, R. Bishop, A. Parkinson, and W. Price, eds., pp. 37–54.
[39] Clauss, G., and Kühnlein, W., 1997, "Simulation of Design Storm Wave Conditions With Tailored Wave Groups," *Proceedings of the Seventh International Offshore and Polar Engineering Conference (ISOPE)*, Honolulu, HI, pp. 228–237.
[40] Clauss, G. F., 2009, "Freak Waves and Their Interaction With Ships and Offshore Structures," *Advances in Numerical Simulation of Nonlinear Water Waves*, (Advances in Coastal and Ocean Engineering), Q. W. Ma, ed., Vol. 11, World Scientific, London, pp. 641–687.

[41] Gonzáles Sánches, S., Gonzáles Prelic, N., and Garcia Galan, S., 1996, "Uvi-Wave, Wavelet Toolbox for Use With MATLAB," Tech. Report.
[42] Rowan, T., 1990, "Functional Stability Analysis of Numerical Algorithms," Ph.D. thesis, University of Texas at Austin, Austin, TX.
[43] Stansberg, C. T., 1997, "On the Nonlinear Behaviour of Ocean Wave Groups," Waves 97: The Third International Symposium on Ocean Wave Measurement and Analysis, Virginia Beach, VA.
[44] Kjeldsen, S. P., 1983, "Determination of Severe Wave Conditions for Ocean Systems in a 3-Dimensional Irregular Seaway," Contribution to the Eighth Congress of the Pan-American Institute of Naval Engineering, pp. 1–35.
[45] Kjeldsen, S. P., and Myrhaug, D., 1979, "Breaking Waves in Deep Water and Resulting Wave Forces," *Proceedings of the 11th Offshore Technology Conference*, Houston, TX, Paper No. oTC 3646, pp. 2515–2521.